

Theory of the Vibrations of Dilute Alloys with Short-Range Order*

W. M. HARTMANN

Argonne National Laboratory, Argonne, Illinois 60439

(Received 4 December 1967)

Using thermally averaged double-time Green's functions, we develop a theory to calculate the effect of a small concentration of nonrandom mass defects on the vibrational properties of a monatomic crystal. The low-concentration approximation used is shown to be equivalent to that used by Elliott and Taylor for the random-impurity case, correct to first order but only approximately correct to higher orders in the concentration. This simple theory is used to find a shift of the resonant or local-mode peak due to short-range order among defects, which might be seen by infrared absorption in imperfect insulators. The integrated absorption is shown to be independent of the ordering for charged defects, but not for uncharged defects which induce optical absorption through atomic deformations. The general expression derived for the inelastic coherent neutron scattering cross section includes a branch-mixing term which disappears for scattering vectors of high symmetry. Using the Debye approximation (for which the cross section can be written in a self-energy form) and the appropriate short-range order parameters from the linear theory of Clapp and Moss, we calculate the shifts and widths of the neutron scattering peaks for $\text{Cu}_{0.997}\text{Au}_{0.003}$. The agreement with the experimental results of Svensson, Brockhouse, and Rowe is not good. A small clustering of light mass defects, represented approximately by nearest-neighbor correlations, is shown to broaden a low-frequency impurity band but to have relatively little effect on a high-frequency local mode.

I. INTRODUCTION

WHEN defects are introduced into a crystal, striking changes in the vibrational properties of the crystal may occur. Vibrational modes may appear at frequencies above the band of perfect-crystal vibration frequencies, or the band itself may be altered. These effects have been observed experimentally in measurements of the infrared absorption coefficient and neutron scattering cross sections. Their thermodynamic consequences have been apparent in measurements of specific heat, thermal conductivity, and thermopower. On the whole, the theories of imperfect-crystal vibrations which have been developed are successful in explaining the general features of a wide variety of experiments when the defect atom concentration c is low and when the effect of a single defect extends only to the nearest or second-nearest neighbors. In the simplest approximation, a foreign substitutional atom is treated as an isolated mass defect with force constants unchanged.

The Green's-function theory provides a way to sum exactly all the phonon scatterings from a single defect. At finite defect concentrations, however, the interference between phonons scattered by different defects may become important. Since Dyson's¹ paper on the vibrations of a disordered harmonic chain, many authors have tried to account for these interference effects in one, two, and three dimensions.² Recently, Payton and Visscher³ have performed extensive computer calculations for three-dimensional crystals, and Elliott and Taylor,⁴ and Taylor⁵ have derived approxi-

mate analytic theories for calculating the thermal averages of physical properties of realistic imperfect crystals.

So far as we know, no general theory has been given without the assumption that the defects are randomly distributed in the crystal, although correlations between nearest-neighbor defects have been included in a computation of the moments of the frequency spectrum of a linear chain⁶ and in a calculation of the normal-mode frequencies of β -brass to second order in perturbations on a mean crystal.⁷ At large concentrations of defects, of course, many alloys become ordered, and a proper theory would begin with the stoichiometric alloy rather than with the pure solvent crystal. Even at defect concentrations well below the ideal concentration, the defects may tend to order themselves to approximate the arrangement of an ordered phase close to the given concentration on the phase diagram.

The theory developed in this paper involves a low-concentration expansion, but allows for possible short-range order among the defects as can be measured by x-ray diffraction. The theory is useful then for those concentrations that are low enough for a low-concentration expansion to apply yet high enough for some ordering of the defects to occur over short ranges. The nonrandom defect distribution is introduced through a defect pair correlation function $\rho_{l_1 l_2}$, which depends only on unit cell indices. For presentation, we have taken the simplest such case, mass defects in a monatomic cubic crystal, but the theory is directly applicable to any problem in which the mass defects can be considered as segregated onto one particular site of the unit cell. Mass defects in alkali halides and III-IV compounds could thus be treated directly, whereas defects in diamond or anion defects in alkaline-earth halides would require a somewhat more complicated formalism with a site-dependent ρ .

* Based on work performed under the auspices of the U. S. Atomic Energy Commission.

¹ F. J. Dyson, *Phys. Rev.* **92**, 1331 (1953).

² See the review by A. A. Maradudin, in *Solid State Physics*, edited by F. Seitz and D. Turnbull (Academic Press Inc., New York, 1966), Vol. 18, p. 273 ff.

³ D. N. Payton and W. M. Visscher, *Phys. Rev.* **154**, 802 (1967); **156**, 1032 (1967).

⁴ R. J. Elliott and D. W. Taylor, *Proc. Roy. Soc. (London)* **296**, 161 (1967). This paper will be referred to as ET.

⁵ D. W. Taylor, *Phys. Rev.* **156**, 1017 (1967).

⁶ Y. Fukuda and K. Yoshida, *J. Phys. Soc. Japan* **17**, 920 (1962).

⁷ P. J. Wojtowicz and J. G. Kirkwood, *J. Chem. Phys.* **33**, 1299 (1960).

II. GREEN'S-FUNCTION METHOD

We shall use the double-time thermodynamic Green's functions reviewed by Zubarev⁸ and first applied to lattice dynamics by Elliott and Taylor.⁹ The time Fourier transform of the thermally averaged $\langle \cdots \rangle_T$ displacement correlation function, from which physical properties may be immediately calculated, is given by

$$\int_{-\infty}^{\infty} \langle u_{l\alpha}(t) u_{l'\beta}(t') \rangle_T e^{i\omega(t-t')} d(t-t') \equiv \lim_{\phi \rightarrow 0} 2\pi \hbar n(\omega) \times \text{Im}[G_{ll'\alpha\beta}(\omega - i\phi) - G_{ll'\alpha\beta}(\omega + i\phi)], \quad (1)$$

where $u_{l\alpha}(t)$ is the displacement in the α th direction of the atom l at time t , $G_{ll'\alpha\beta}(\omega)$ is the retarded Green's function of the imperfect crystal, and $n(\omega) = [\exp(\hbar\omega/kT) - 1]^{-1}$.

Using a harmonic Hamiltonian, Elliott and Taylor have derived a general equation of motion in time t expressing the imperfect-crystal Green's function in terms of the analogous perfect-crystal Green's function $P_{ll'\alpha\beta}(\omega)$ and a defect matrix \mathbf{C} :

$$G_{ll'\alpha\beta}(\omega) = P_{ll'\alpha\beta}(\omega) + \sum_{l_1 l_2 \gamma \delta} P_{ll_1 \alpha \gamma}(\omega) C_{l_1 l_2 \gamma \delta} G_{l_2 l' \delta \beta}(\omega), \quad (2)$$

or¹⁰

$$\mathbf{G} = \mathbf{P} + \mathbf{P} \mathbf{C} \mathbf{G}.$$

Considering the system evolution in time t' gives

$$\mathbf{G} = \mathbf{P} + \mathbf{G} \mathbf{C} \mathbf{P}. \quad (3)$$

For the monatomic crystal,

$$P_{ll'\alpha\beta}(\omega) = \frac{1}{mN} \sum_{j\mathbf{k}} \frac{\sigma_{\alpha}^{j\dagger}(\mathbf{k}) \sigma_{\beta}^j(\mathbf{k})}{\omega^2 - \omega_j^2(\mathbf{k})} e^{-i\mathbf{k} \cdot (\mathbf{r}_l - \mathbf{r}_{l'})}. \quad (4)$$

Here, $\sigma_{\alpha}^j(\mathbf{k})$ is an eigenvector of the perfect-crystal dynamical matrix \mathbf{D} , i.e.,

$$\sum_{\beta} D_{\alpha\beta}(\mathbf{k}) \sigma_{\beta}^j(\mathbf{k}) = \omega_j^2(\mathbf{k}) \sigma_{\alpha}^j(\mathbf{k}), \quad (5)$$

and by symmetry the perfect-crystal Green's function depends only on the difference $(\mathbf{r}_l - \mathbf{r}_{l'})$ between the equilibrium positions of the atoms, of mass m , labeled l and l' . The eigenvectors may be chosen to satisfy the orthonormality conditions

$$\sum_j \sigma_{\alpha}^{j\dagger}(\mathbf{k}) \sigma_{\beta}^j(\mathbf{k}) = \delta_{\alpha\beta} \quad (6)$$

and

$$\sum_{\alpha} \sigma_{\alpha}^{j\dagger}(\mathbf{k}) \sigma_{\alpha}^{j'}(\mathbf{k}) = \delta_{jj'}. \quad (7)$$

It is convenient to introduce the Fourier transform

$$P_{\alpha\beta}(\mathbf{k}) \equiv \frac{1}{N} \sum_{ll'} P_{ll'\alpha\beta}(\omega) e^{i\mathbf{k} \cdot (\mathbf{r}_l - \mathbf{r}_{l'})} = -\frac{1}{m} \sum_j \frac{\sigma_{\alpha}^{j\dagger}(\mathbf{k}) \sigma_{\beta}^j(\mathbf{k})}{x - x_j(\mathbf{k})}, \quad (8)$$

where $x \equiv \omega^2$ and $x_j(\mathbf{k}) \equiv \omega_j^2(\mathbf{k})$.

For substitutional defects of mass m' the matrix \mathbf{C} is diagonal:

$$C_{ll'\alpha\beta} \equiv C \delta_{ls} \delta_{l's} \delta_{\alpha\beta} = m \epsilon \omega^2 \delta_{ls} \delta_{l's} \delta_{\alpha\beta}, \quad (9)$$

where

$$\epsilon \equiv \frac{m - m'}{m}, \quad (10)$$

and where s is a member of a collection $\{s_i\}$ of defect sites. Equation (2) may be iterated,

$$\mathbf{G} = \mathbf{P} + \mathbf{P} \mathbf{C} \mathbf{P} + \mathbf{P} \mathbf{C} \mathbf{P} \mathbf{C} \mathbf{P} + \mathbf{P} \mathbf{C} \mathbf{P} \mathbf{C} \mathbf{P} \mathbf{C} \mathbf{P} + \cdots \quad (11)$$

We find a configuration-averaged Green's function $\langle G \rangle$ by averaging each term of (11) over all possible crystals with cN defects in a certain state of short-range order. In the limit of a large number of lattice sites, this configuration average, indicated by brackets $\langle \cdots \rangle$, may be performed by assigning defect occupation probabilities to these sites.

In the second term of (11), there is no possibility of multiple scattering. This term may be represented by graph (a) of Fig. 1,¹¹ and its average over all defect configurations is

$$cC \sum_{l_1} P_{ll_1} P_{l_1 l'}, \quad (12)$$

where we have dropped the Cartesian indices for the moment.

The third term may be represented by graphs (b) and (c); the latter represents a double scattering from the same defect. We introduce the defect correlation function $\rho_{l_1 l_2}$ which gives the following probability: If there is a defect at l_1 , then there is a defect at site l_2 . In a homogeneous crystal, this pair-correlation function is

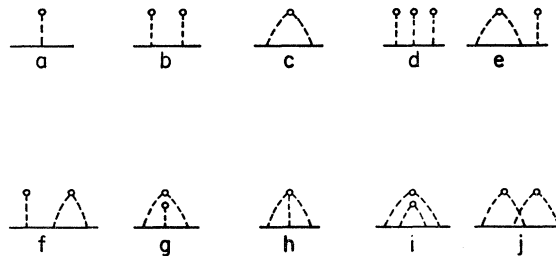


FIG. 1. Impurity scattering graphs. Each dashed line represents a single scattering from one impurity, indicated by a dot. From left to right along the solid horizontal line, dashed lines are in the order of the defect matrices in Eq. (11).

¹¹ These graphs are of the type introduced by J. S. Langer, J. Math. Phys. 2, 584 (1961).

⁸ D. N. Zubarev, Usp. Fiz. Nauk 71, 71 (1960) [English transl.: Soviet Phys.—Usp. 3, 320 (1960)].

⁹ R. J. Elliott and D. W. Taylor, Proc. Phys. Soc. (London) 83, 189 (1964).

¹⁰ In this paper a Green's function without indices G or P will imply the site representation $G_{ll'\alpha\beta}$ or $P_{ll'\alpha\beta}$, where site indices always appear as subscripts. The space Fourier transforms will be written as $G(\mathbf{k})$ or $P(\mathbf{k})$.

simply related to the Warren short-range order parameters α_l used by Cowley¹² and others,

$$\rho_{l_1 l_2} = c + (1-c)\alpha_{(l_1-l_2)}. \quad (13)$$

The value of α_l is the same for all sites l in a given shell λ of atoms around the origin. The third term becomes

$$\begin{aligned} \langle \sum_{l_1 l_2} P_{l_1} C_{l_1 l_1} P_{l_1 l_2} C_{l_2 l_2} P_{l_2 l_2} \rangle \\ = cC^2 \sum_{l_1 l_2} P_{l_1} P_{l_1 l_2} P_{l_2 l_2} \rho_{l_1 l_2}. \end{aligned} \quad (14)$$

Similarly, the fourth term involves $\rho_{l_1 l_2 l_3}$, the probability that if there is a defect at l_1 , then there are defects both at l_2 and l_3 . This term is represented by graphs (d)–(h) of Fig. 1. The n th term in this expansion will involve $\rho_{l_1 l_2 l_3 \dots l_{n-1}}$ defined similarly to $\rho_{l_1 l_2 l_3}$.

We now make the approximation

$$\begin{aligned} c\rho_{l_1 l_2 l_3} &= c\rho_{l_1 l_2} \rho_{l_2 l_3}, \\ c\rho_{l_1 l_2 l_3 l_4} &= c\rho_{l_1 l_2} \rho_{l_2 l_3} \rho_{l_3 l_4}, \\ c\rho_{l_1 l_2 l_3 \dots l_n} &= c\rho_{l_1 l_2} \rho_{l_2 l_3} \dots \rho_{l_{n-1} l_n}. \end{aligned} \quad (15)$$

This approximation has several aspects. The multiplication of pair-correlation functions to obtain higher-order correlation functions is exact only if the pair functions are independent of one another. This multiplicative aspect of (15) is correct then for random-defect crystals and for perfectly ordered crystals. For the short-range-ordered case, the approximation may be justified for small defect concentrations if there is no very strong tendency for defects to cluster. In this case, it can be argued that defects are well separated from one another on the average and pair correlation functions may be taken as independent. The second aspect of approximation (15) is its unphysical asymmetry, which has the effect of weighting properly all uncrossed graphs in the expansion (11) but weighting improperly all crossed graphs. A crossed graph represents a term in (11) in which two or more nonadjacent defect indices are the same, e.g., graph (g) of Fig. 1. This effect may be seen easily in the random limit, where

$$\rho_{l_1 l_2}^{\text{RL}} = c + \delta_{l_1 l_2}(1-c). \quad (16)$$

In this limit, for example, $c\rho_{l_1 l_2 l_3} = c\rho_{l_1 l_2} \rho_{l_2 l_3}$ for all values of l_1, l_2, l_3 except for $l_1 = l_3$ [graph (g)], where the approximation is wrong by a factor c . Generally, the approximated graph for the expression

$$cC^n \sum_{l_1 l_2 \dots l_n} P_{l_1} P_{l_1 l_2} P_{l_2 l_3} \dots P_{l_{n-1} l_n} \rho_{l_1 l_2 l_3 \dots l_n} \quad (17)$$

will be underweighted by a factor c^b , where $b-1$ is the number of changes of defect-site indices along the horizontal line minus the number of defects in the graph. Thus the fourth-order graphs in two defects i and j are underweighted by factors c and c^2 , respectively.

In Appendix A, we show that our approximation (15) is equivalent in the random limit to the approximation of ET derived in a more intuitive way. Additional discussion of both aspects of this approximation appears in Sec. VII.

In the limit of perfectly ordered defects in a stoichiometric alloy, our approximation is exact since all n -defect correlation functions are either 1 or 0. However, the perfect crystal thus represented is still an average crystal, because of the configuration average over the first defect site. For Cu₃Au, for example, the averaging distributes the heavy gold defect evenly over the four sites in the unit cell. The symmetry of the perfect copper crystal is restored and it is not possible with this technique to leap from one crystal type to another.

With this approximation, we may sum all the terms of Eq. (11). We define

$$\rho(\mathbf{k}) = \sum_l \rho_{0l} e^{i\mathbf{k} \cdot \mathbf{r}_l}, \quad (18)$$

and using (4) and summing over internal l indices, we find that

$$\begin{aligned} \langle G_{ll' \alpha \beta}(\omega) \rangle &= P_{ll' \alpha \beta}(\omega) + \frac{cC}{N} \sum_{\gamma \mathbf{k}} P_{\alpha \gamma}(\mathbf{k}) \left[\sum_{n=0}^{\infty} \left(\frac{C}{N} \sum_{\mathbf{k}'} P(\mathbf{k}') \right. \right. \\ &\quad \left. \left. \times \rho(\mathbf{k} - \mathbf{k}') \right)^n \right]_{-\gamma \mathbf{k}} P_{\beta \gamma}(\mathbf{k}) e^{-i\mathbf{k} \cdot (\mathbf{r}_l - \mathbf{r}_{l'})}. \end{aligned} \quad (19)$$

If the sum is performed,

$$\begin{aligned} \langle G_{ll' \alpha \beta}(\omega) \rangle &= P_{ll' \alpha \beta}(\omega) \\ &+ \frac{cC}{N} \sum_{\gamma \mathbf{k}} P_{\alpha \gamma}(\mathbf{k}) Z_{\gamma \beta}(\mathbf{k}) P_{\beta \gamma}(\mathbf{k}) e^{-i\mathbf{k} \cdot (\mathbf{r}_l - \mathbf{r}_{l'})}, \end{aligned} \quad (20)$$

where

$$\mathbf{Z}(\mathbf{k}) \equiv \left[1 - \frac{C}{N} \sum_{\mathbf{k}'} \mathbf{P}(\mathbf{k}') \rho(\mathbf{k} - \mathbf{k}') \right]^{-1}. \quad (21)$$

The transformation

$$T_{\alpha}^j(l, \mathbf{k}) \equiv (m/N)^{1/2} \sigma_{\alpha}^j(\mathbf{k}) e^{-i\mathbf{k} \cdot \mathbf{r}_l} \quad (22)$$

selects a particular mode with wave vector \mathbf{k} and branch j from the perfect-crystal Green's function,

$$\begin{aligned} \sum_{ll' \alpha \beta} T_{\alpha}^{j\dagger}(l, \mathbf{k}) P_{ll' \alpha \beta}(\omega) T_{\beta}^{j'}(l', \mathbf{k}') \\ = \frac{\delta_{jj'} \delta(\mathbf{k} \mathbf{k}')}{x - x_j(\mathbf{k})} \equiv P_{jj'}(\mathbf{k} \mathbf{k}'). \end{aligned} \quad (23)$$

The normal modes of an imperfect crystal are not specified by a single wave vector. Such experiments as inelastic neutron scattering and optical absorption do, however, look for the response of a system at a particular wave vector. Since we have restored the translational symmetry of the perfect crystal, we find that

$$\langle G_{jj'}(\mathbf{k} \mathbf{k}') \rangle = \sum_{ll' \alpha \beta} T_{\alpha}^{j\dagger}(l, \mathbf{k}) \langle G_{ll' \alpha \beta}(\omega) \rangle T_{\beta}^{j'}(l', \mathbf{k}') \quad (24)$$

¹² J. M. Cowley, Phys. Rev. 77, 669 (1950).

is diagonal on \mathbf{k} :

$$\langle G_{jj'}(\mathbf{k}\mathbf{k}') \rangle = \delta(\mathbf{k}\mathbf{k}') \{ \delta_{jj'} P_j(\mathbf{k}) + c\epsilon x P_j(\mathbf{k}) Z_{jj'}(\mathbf{k}) P_{j'}(\mathbf{k}) \}, \quad (25)$$

where we define

$$Z_{jj'}(\mathbf{k}) \equiv \sum_{\alpha\beta} \sigma_{\alpha}^j(\mathbf{k}) Z_{\alpha\beta}(\mathbf{k}) \sigma_{\beta}^{j'\dagger}(\mathbf{k}). \quad (26)$$

In general, the correlations between defect sites mix the branches of the crystal vibrations.

The above Green's function $\langle \mathbf{G} \rangle$ represents the response of a crystal to a probe which interacts with both host and defect atoms in the same way. In the more usual situation, defect and host atoms interact differently. The defect and host atoms may have a different effective charge and thus interact differently with light; they may have different neutron scattering lengths. Therefore, we need to find conditionally averaged Green's functions, $G_{ll'\alpha\beta}^d(\omega)$ and $G_{ll'\alpha\beta}^{dd}(\omega)$, where, respectively, the first site and both sites are occupied by defect atoms. We define

$$\mathbf{G}^d \equiv (1/C) \langle \mathbf{C}\mathbf{G} \rangle. \quad (27)$$

The average of Eq. (2) gives

$$\langle \mathbf{G} \rangle = \mathbf{P} + \mathbf{P}\mathbf{C}\mathbf{G}^d \quad (28)$$

or

$$\langle G_{jj'}(\mathbf{k}\mathbf{k}') \rangle = \delta_{jj'} \delta(\mathbf{k}\mathbf{k}') P_j(\mathbf{k}) + \epsilon x P_j(\mathbf{k}) G_{jj'}^d(\mathbf{k}\mathbf{k}') \quad (29)$$

upon transformation. Comparing Eqs. (25) and (29), we find that

$$G_{jj'}^d(\mathbf{k}\mathbf{k}') = \delta(\mathbf{k}\mathbf{k}') c P_j(\mathbf{k}) Z_{jj'}(\mathbf{k}). \quad (30)$$

If Eqs. (2) and (3) are combined and averaged as

$$\langle \mathbf{G} \rangle = \mathbf{P} + \mathbf{P}\langle \mathbf{C} \rangle \mathbf{P} + \mathbf{P}\langle \mathbf{C}\mathbf{G}\mathbf{C} \rangle \mathbf{P} \quad (31)$$

and

$$\mathbf{G}^{dd} \equiv (1/C^2) \langle \mathbf{C}\mathbf{G}\mathbf{C} \rangle, \quad (32)$$

then

$$\langle G_{jj'}(\mathbf{k}\mathbf{k}') \rangle = \delta_{jj'} \delta(\mathbf{k}\mathbf{k}') [P_j(\mathbf{k}) + c\epsilon x P_j^2(\mathbf{k}) + \epsilon^2 x^2 P_j(\mathbf{k}) G_{jj'}^{dd}(\mathbf{k}\mathbf{k}') P_{j'}(\mathbf{k}')] \quad (33)$$

If Eq. (19) is written with the $n=0$ term explicitly included and the remaining terms summed, it may be compared with Eq. (33) and

$$G_{jj'}^{dd}(\mathbf{k}\mathbf{k}') = \delta(\mathbf{k}\mathbf{k}') (c/\epsilon x) [Z_{jj'}(\mathbf{k}) - \delta_{jj'}]. \quad (34)$$

In \mathbf{G}^d the first site is necessarily a defect, but since the second site must be either a defect or a *host* atom,

$$\mathbf{G}^d = \mathbf{G}^{dd} + \mathbf{G}^{dh}. \quad (35)$$

Similarly,

$$\mathbf{G}^h = \mathbf{G}^{hd} + \mathbf{G}^{hh} \quad (36)$$

and

$$\langle \mathbf{G} \rangle = \mathbf{G}^d + \mathbf{G}^h. \quad (37)$$

From Eqs. (30) and (34), then,

$$G_{jj'}^{dh}(\mathbf{k}\mathbf{k}') = G_{jj'}^{hd}(\mathbf{k}\mathbf{k}') = \delta(\mathbf{k}\mathbf{k}') (c/\epsilon x) \times \{ \delta_{jj'} + Z_{jj'}(\mathbf{k}) [\epsilon x P_j(\mathbf{k}) - 1] \} \quad (38)$$

and

$$G_{jj'}^{hh}(\mathbf{k}\mathbf{k}') = [\delta(\mathbf{k}\mathbf{k}')/\epsilon x] \{ [\epsilon x P_j(\mathbf{k}) - c] \delta_{jj'} + c Z_{jj'}(\mathbf{k}) [\epsilon x P_j(\mathbf{k}) - 1] [\epsilon x P_{j'}(\mathbf{k}) - 1] \}. \quad (39)$$

These Green's functions will be diagonal on j if $Z_{\alpha\beta}(\mathbf{k})$ is diagonal on α with all three diagonal elements equal, and also in the case of the random limit.

III. OPTICAL ABSORPTION

If defects with a charge e are introduced into a covalent crystal of volume V , only the defects will interact with light in the harmonic-rigid-atom approximation.¹³ Because of its relatively long wavelength, infrared radiation with velocity ηv and transverse polarization vector \mathbf{t} is absorbed only by the response of a crystal at $\mathbf{k}=0$ and the absorption coefficient is

$$K(\omega) = \frac{4\pi\omega N e^2 \Lambda}{\eta v V m} \text{Im} \sum_j [\mathbf{t} \cdot \boldsymbol{\sigma}^j(0)]^2 G_j^{dd}(0), \quad (40)$$

where Λ is a local field correction $\equiv [\frac{1}{3}(\eta^2 + 2)]^2$. In this limit,

$$Z_{\gamma\delta}(0) = \left\{ 1 - \frac{\epsilon x}{N} \sum_{j'\mathbf{k}'} \frac{\boldsymbol{\sigma}^{j'\dagger}(\mathbf{k}') \boldsymbol{\sigma}^{j'}(\mathbf{k}')}{x - x_{j'}(\mathbf{k}')} \rho(-\mathbf{k}') \right\}_{\gamma\delta}^{-1}. \quad (41)$$

The above sum over wave vectors \mathbf{k}' may be separated into a sum of sums over a star of \mathbf{k} values constructed by operating on a particular \mathbf{k} with the rotation elements of the perfect crystal space group; $x_j(\mathbf{k})$ and $\rho(\mathbf{k}) [= \rho(-\mathbf{k})]$ are then the same for any \mathbf{k} in the star. For crystals of cubic symmetry, every star sum of the form

$$\sum_{\mathbf{k}}^* \sigma_x^{j\dagger}(\mathbf{k}) \sigma_y^j(\mathbf{k}) \quad (42)$$

vanishes unless x and y are the same and

$$Z_{\gamma\delta}(0) = \delta_{\gamma\delta} \left\{ 1 - \frac{\epsilon x}{3N} \sum_{j'\mathbf{k}'} \frac{\rho(\mathbf{k}')}{x - x_{j'}(\mathbf{k}')} \right\}^{-1}. \quad (43)$$

Then, manipulating Eq. (34) and discarding terms proportional to the perfect-monatomic-crystal Green's functions which give no absorption, we find that

$$K(\omega) = \frac{4\pi\omega N e^2 \Lambda}{\eta v V m} \text{Im} \left[\left(\frac{c(1-c)}{3N} \sum_{j\mathbf{k}} \alpha(\mathbf{k}) P_j(\mathbf{k}) \right) / \left(1 - \frac{(1-c)\epsilon x}{3N} \sum_{j'\mathbf{k}'} \alpha(\mathbf{k}') P_{j'}(\mathbf{k}') \right) \right], \quad (44)$$

where we have used the Fourier transform of (13)

$$\rho(\mathbf{k}) = cN\delta(\mathbf{k}) + (1-c)\alpha(\mathbf{k}). \quad (45)$$

¹³ The assumption that only the defect contributes to the optical absorption has recently been criticized by R. S. Leigh and B. Szigeti, Proc. Roy. Soc. (London) **A301**, 211 (1967); Phys. Rev. Letters **19**, 566 (1967).

The effect of the correlations between defects can be seen by rewriting (44) as

$$K = \frac{4\pi N e^2 \Delta c (1-c)}{\eta v V m} \text{Im} \left[m \omega \sum_l \alpha_l P_{0l}(\omega) / (1 - (1-c)m\epsilon\omega^2 \sum_l \alpha_l P_{0l}(\omega)) \right]. \quad (46)$$

The zeros of the denominator give the frequencies x_R of localized modes for light mass defects and the frequencies of resonances in the band for heavy mass defects where optical absorption peaks should occur. Since α_0 is always equal to 1, and since all other α_l are zero for the random defect arrangement, it appears that the correlation between defects result in a shift of the peak from x_R . If the shift Δx_R is small compared to x_R ,

$$\frac{\Delta x_R}{x_R} = \frac{\sum_{l \neq 0} \alpha_l P_{0l}(x_R)}{\mathcal{P} \sum_{jk} \alpha(\mathbf{k}) x_j(\mathbf{k}) / [x_R - x_j(\mathbf{k})]^2}, \quad (47)$$

where \mathcal{P} indicates that the principal part is to be taken. The total integrated absorption, however, is independent of the defect correlations. Because the imaginary part in Eq. (44) is even in ω , the net absorption is temperature-independent, and the integrated absorption is given by the half of the integral of (44) from minus to plus infinity. The conjugate real part of this integral is zero, and the imaginary part is given by half the integral clockwise around the contour at infinity enclosing all the poles in and out of the band.

$$\begin{aligned} \bar{K} &\equiv \int_0^\infty K(\omega) d\omega = \lim_{\varphi \rightarrow 0} \frac{1}{2} \int_{-\infty}^\infty K(\omega + i\varphi) d\omega \\ &= \frac{1}{4} \int_{\mathcal{C}} K(\omega) d\omega. \end{aligned} \quad (48)$$

However, from (4) and (6),

$$\lim_{\omega \rightarrow \infty} P_{0l\alpha\beta}(\omega) = \frac{1}{m\omega^2} \delta_{0l} \delta_{\alpha\beta}, \quad (49)$$

and, since $\alpha_0 = 1$,

$$\bar{K} = \frac{2\pi^2 N e^2 c (1-c) \Delta}{\eta v V m [1 - (1-c)\epsilon]}. \quad (50)$$

A similar result can be expected to hold in the more useful case of diatomic crystals such as diamond.

For uncharged but polarizable mass defects randomly distributed in a rare gas crystal, it was found¹⁴ that the optical absorption was given by an expression like Eq. (40) with an effective defect charge proportional to the square of the frequency. If short-range order is included, the optical absorption to first order in c is of the

form

$$K(\omega) = c\gamma\omega^5 \text{Im} \left[\left(\frac{1}{3N} \sum_{jk} [\omega^2 - \omega_j^2(\mathbf{k})]^{-1} \alpha(\mathbf{k}) \right) / \left(1 - \frac{\epsilon\omega^2(1-c)}{3N} \sum_{j'k'} [\omega^2 - \omega_{j'}^2(\mathbf{k}')]^{-1} \alpha(\mathbf{k}') \right) \right], \quad (51)$$

where γ is a constant depending on the parameters of the model used. The integrated absorption in the random case depended on the second and fourth moments of the perfect-crystal frequency spectrum. A similar expression results from the ordered case, except that the moments required are those of the spectral function weighted with $\alpha(\mathbf{k})$. To first order in c ,

$$\bar{K} = \frac{c\gamma\pi}{2(1-\epsilon)^2} \left\{ (\omega^4)_{\text{av}} + \frac{\epsilon}{1-\epsilon} [(\omega^2)_{\text{av}}]^2 \right\}, \quad (52)$$

where

$$(\omega^2)_{\text{av}} \equiv \frac{1}{3N} \sum_{jk} \alpha(\mathbf{k}) \omega_j^2(\mathbf{k}) = \sum_l D_{0lx} \alpha_l, \quad (53)$$

$$(\omega^4)_{\text{av}} \equiv \frac{1}{3N} \sum_{jk} \alpha(\mathbf{k}) \omega_j^4(\mathbf{k}) = \sum_{ll'\gamma} D_{0lx} \gamma \alpha_{(l-l')} D_{l'0\gamma x}. \quad (54)$$

In the last step, (5) has been used. The dipole moments induced on the defect atom depend upon the nature of the neighboring atoms. The optical absorption is weighted more strongly at high frequencies where neighboring atoms have opposing motions, and the integrated absorption is not independent of the order.

IV. NEUTRON SCATTERING

The most complete information about a vibrating system can be obtained from measurements of the inelastic cross section for scattering neutrons with an initial wave vector \mathbf{k}_1 to a final wave vector $\mathbf{k}_2 \equiv \mathbf{k}_1 + \mathbf{Q}$ with a neutron energy gain of $\hbar\omega$.

$$\frac{\partial^2 \sigma}{\partial \Omega \partial \omega} = \frac{k_2}{k_1} S(\mathbf{Q}, \omega). \quad (55)$$

In the harmonic approximation, the Van Hove function $S(\mathbf{Q}, \omega)$ may be transformed to¹⁵

$$S(\mathbf{Q}, \omega) = \frac{2\hbar n(\omega)}{N} \left\langle \left\langle \sum_{l'l''\alpha\beta} A_l A_{l''} e^{i\mathbf{k} \cdot (\mathbf{r}_l - \mathbf{r}_{l''})} Q_\alpha Q_\beta \times \text{Im} G_{ll''\alpha\beta}(\omega) \right\rangle \right\rangle_N. \quad (56)$$

The effective scattering length of the atom at site l is the usual atomic scattering length a_l multiplied by an atomic Debye-Waller factor,

$$A_l = a_l e^{-\frac{1}{2} \langle (\mathbf{Q} \cdot \mathbf{u}_l)^2 \rangle_T}. \quad (57)$$

The brackets in Eq. (56) indicate a configuration aver-

¹⁴ W. M. Hartmann and R. J. Elliott, Proc. Phys. Soc. (London) 91, 187 (1967).

¹⁵ C. Kittel, *Quantum Theory of Solids* (John Wiley & Sons, Inc., New York, 1963), p. 394 ff.

age over the defect sites of the imperfect crystal and the brackets $\langle \dots \rangle_N$ indicate an average over nuclear isotopes and spin states. In the exponent, the wave-vector transfer \mathbf{Q} has been reduced by an appropriate reciprocal-lattice vector to place $\mathbf{\kappa}$ in the perfect-crystal first Brillouin zone,

$$\mathbf{\kappa} = \mathbf{Q} - \boldsymbol{\tau}. \quad (58)$$

The averages above may be taken, and from the definitions (27) and (32),

$$S(\mathbf{Q}, \omega) = \frac{2\hbar n(\omega)}{m} \sum_{jj'} \sum_{\alpha\beta} Q_{\alpha} \sigma_{\alpha}^{jj'}(\mathbf{\kappa}) Q_{\beta} \sigma_{\beta}^{jj'}(\mathbf{\kappa}) \\ \times \text{Im} \{ \langle A_h \rangle_N^2 G_{jj'}^{hh}(\mathbf{\kappa}) + 2 \langle A_d \rangle_N \langle A_h \rangle_N G_{jj'}^{dh}(\mathbf{\kappa}) \\ + \langle A_d \rangle_N^2 G_{jj'}^{dd}(\mathbf{\kappa}) \} + S_{\text{inc}}(\mathbf{Q}, \omega). \quad (59)$$

The incoherent term is

$$S_{\text{inc}}(\mathbf{Q}, \omega) = \frac{2\hbar n(\omega)}{m} \sum_{\alpha\beta} Q_{\alpha} Q_{\beta} \\ \times \text{Im} \{ \alpha_h^2 \langle G_{00\alpha\beta}(\omega) \rangle + (\alpha_d^2 - \alpha_h^2) G_{00\alpha\beta}^d(\omega) \}, \quad (60)$$

where the incoherent scattering lengths are defined as

$$\alpha^2 \equiv \langle A^2 \rangle_N - \langle A \rangle_N^2. \quad (61)$$

Upon substitution of Eqs. (34), (38), and (39) into (59) for the coherent scattering,

$$S_{\text{coh}}(\mathbf{Q}, \omega) = \frac{2\hbar n(\omega)}{m} \sum_{jj'} [\mathbf{Q} \cdot \boldsymbol{\sigma}^j(\mathbf{\kappa})][\mathbf{Q} \cdot \boldsymbol{\sigma}^{j'}(\mathbf{\kappa})] \\ \times \text{Im} \left\{ \delta_{jj'} \langle A_h \rangle_N^2 P_j(\mathbf{\kappa}) + \frac{c}{\epsilon x} Z_{jj'}(\mathbf{\kappa}) [(\epsilon x P_j(\mathbf{\kappa}) - 1) \langle A_h \rangle_N \right. \\ \left. + \langle A_d \rangle_N] [(\epsilon x P_{j'}(\mathbf{\kappa}) - 1) \langle A_h \rangle_N + \langle A_d \rangle_N] \right\}. \quad (62)$$

A typical constant- \mathbf{Q} neutron scattering experiment compares the plots of scattering intensity versus energy transfer at a particular \mathbf{Q} value for perfect and imperfect crystals. In the perfect crystal the neutrons gain energy from the destruction of phonons of a particular branch and of wave vector $\mathbf{\kappa}$. In the case of an imperfect crystal with mass defects randomly distributed, the observed response of the crystal to a probe of wave vector $\mathbf{\kappa}$ is a combination of phonons, all from the same branch. Correlations among the defects, however, are seen to mix the branches of the perfect crystal in Eq. (62). In addition, the mixing of branches prevents $\langle G_{00\alpha\beta} \rangle$ and $G_{00\alpha\beta}^d$ from being diagonal and the broad incoherent background will no longer depend simply on Q^2 but will show some dependence on scattering angle.

V. COPPER-GOLD ALLOY

Svensson, Brockhouse, and Rowe¹⁶ have measured the inelastic neutron scattering cross section for copper

¹⁶ E. C. Svensson, B. N. Brockhouse, and J. M. Rowe, *Solid State Commun.* **3**, 245 (1965).

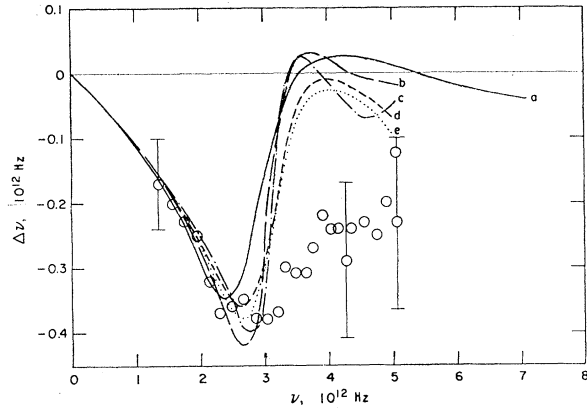


FIG. 2. The shift of the frequency of the transverse response of a $\text{Cu}_{0.997}\text{Au}_{0.003}$ crystal at $\mathbf{Q} = [22\kappa]$ from its value for pure Cu plotted as a function of the perfect-crystal response frequency. Curves are theoretical predictions of the Debye model for (a) random defects, (b) ten shells of ordered defects with short-range order characterized by a temperature $T = T_c/0.7$, (c) ten shells at $T = T_c/0.95$, (d) two shells at $T = T_c/0.9$, (e) two shells at $T = T_c/0.95$. The zeros of the random curve differ slightly from those in the equivalent plot by Svensson *et al.* due to the factor $(1-c)$ in Eq. (74). Circles are the data taken from E. C. Svensson, Ph.D. thesis, McMaster University, 1967 (unpublished), for the alloy at room temperature.

with 9.3 at. % gold impurities. They have analyzed their results in terms of the low-concentration theory of Elliott and Maradudin,¹⁷ in which the gold defects produce a shift and width of the perfect-crystal one-phonon lines. The scattering, which destroys a phonon in branch j , is then proportional to a modified δ -function expression,

$$S_{\text{coh}}^j(\mathbf{Q}, \omega) \propto \text{Im} \frac{1}{\omega^2 - \omega_j^2(\mathbf{\kappa}) - \omega^2 \Sigma(\omega)}, \quad (63)$$

where $\omega \Sigma(\omega)$ is a self-energy with real and imaginary parts, giving the shift and width, respectively,

$$\Sigma(\omega) \equiv \Delta(\omega) + i\Gamma(\omega). \quad (64)$$

The experimental results and the predictions of this random mass defect theory are given in Fig. 2. Despite the large error bars at high frequencies, it appears that the simple theory does not account for the experimental results. In particular, the experiments do not show the positive energy shift predicted by the theory. One might argue that the low-concentration theory should not work very well at defect concentrations as high as 9.3%. The higher-concentration work of Taylor,⁵ however, suggests that the discrepancy between theory and experiment is not a simple concentration effect. Behera and Deo¹⁸ actually find that their higher-concentration

¹⁷ R. J. Elliott and A. A. Maradudin, in *Symposium on Inelastic Scattering of Neutrons* (International Atomic Energy Agency, Vienna, 1964), Vol. I, p. 231. Several of the results obtained by Elliott and Maradudin are also implicitly contained in earlier work by Russian authors; e.g., Yu. Kagan and Ya. A. Iosilevskii, *Zh. Eksperim. i Teor. Fiz.* **44**, 1375 (1963) [English transl.: *Soviet Phys.—JETP* **17**, 925 (1963)], and the references contained therein.

¹⁸ S. N. Behera and B. Deo, *Phys. Rev.* **153**, 728 (1967).

theory shifts the emergence of positive energy shifts to a lower frequency. It would be possible to provide better agreement with experiment with a theory that took into account force-constant changes between defects and their neighbors, but the relatively good agreement between the random mass defect theory and the experimental results on copper with 3 at.% gold defects¹⁹ suggests that force-constant changes may not be the dominant contribution to the discrepancy in the 9.3% case.

The low-concentration theory of this paper is not strictly valid at 9.3%, although it might be expected to predict correctly the qualitative features in this case. At 25% gold concentration copper-gold forms a well-ordered simple cubic alloy below 390°K with gold on the corners and copper on the faces. It seems very likely that there is a considerable remnant of this order over short ranges at 9.3% concentration. The coherent scattering lengths of copper and gold are virtually identical. At room temperature $T_m/T=1.2$ and the mean-square displacements of copper and gold atoms are essentially the same. To a good approximation, then

$$\langle A_h \rangle_N = \langle A_d \rangle_N \equiv A \quad (65)$$

and

$$S_{\text{coh}}(\mathbf{Q}, \omega) = \frac{2\hbar n(\omega)A^2}{m} \sum_{jj'} [\mathbf{Q} \cdot \boldsymbol{\sigma}^j(\mathbf{k})][\mathbf{Q} \cdot \boldsymbol{\sigma}^{j'}(\mathbf{k})] \times \text{Im} G^{jj'}(\mathbf{k}). \quad (66)$$

We may make this equation resemble the self-energy form of Elliott and Maradudin by using (25), (26), (21), and (45), and performing some algebra,

$$S_{\text{coh}}(\mathbf{Q}, \omega) = \frac{2\hbar n(\omega)A^2}{m} \sum_{jj'} [\mathbf{Q} \cdot \boldsymbol{\sigma}^j(\mathbf{k})][\mathbf{Q} \cdot \boldsymbol{\sigma}^{j'}(\mathbf{k})] \times \text{Im} \left\{ \left[x - x_j(\mathbf{k}) \right] \delta_{jj'} - c\epsilon x \frac{x - x_j(\mathbf{k})}{x - x_{j'}(\mathbf{k})} \left[\delta_{jj'} - \frac{(1-c)C}{N} \times \sum_{\alpha, \beta, \mathbf{k}} \sigma_{\alpha}^j(\mathbf{k}) P_{\alpha\beta}(\mathbf{k}) \sigma_{\beta}^{j'}(\mathbf{k}) \alpha(\mathbf{k} - \mathbf{k}) \right]^{-1} \right\}^{-1}. \quad (67)$$

Because of the branch mixing, it is not generally possible to attain a simple self-energy form. As in the case of force-constant changes, however, the self-energy is diagonal on j for certain \mathbf{k} vectors along symmetry axes, although the self-energy still depends on j and \mathbf{k} , and not just on ω .

For the degenerate transverse branches studied experimentally at $\mathbf{Q}=[22\kappa]$ the vector \mathbf{k} is along the crystal z axis. We may show that off-diagonal elements of $Z_{\alpha\beta}(\mathbf{k})$ are zero by a \mathbf{k} -star sum argument, if we limit the star to those wave vectors created by operating on a particular \mathbf{k} value with only those operations of the cubic group that leave the z coordinate unchanged.

This star is large enough to ensure that for every \mathbf{k} in the star there will be other vectors, \mathbf{k}_1 and \mathbf{k}_2 , in the star, for which

$$\sigma_x^j(\mathbf{k}) = -\sigma_x^j(\mathbf{k}_1), \quad \sigma_y^j(\mathbf{k}) = \sigma_y^j(\mathbf{k}_1), \quad \sigma_z^j(\mathbf{k}) = \sigma_z^j(\mathbf{k}_1), \quad (68)$$

and

$$\sigma_x^j(\mathbf{k}) = \sigma_x^j(\mathbf{k}_2), \quad \sigma_y^j(\mathbf{k}) = -\sigma_y^j(\mathbf{k}_2), \quad \sigma_z^j(\mathbf{k}) = \sigma_z^j(\mathbf{k}_2).$$

Since $\rho(\mathbf{k} - \mathbf{k})$ or $\alpha(\mathbf{k} - \mathbf{k})$ is invariant under this limited set of operations, we find that

$$Z_{\alpha\beta}(\mathbf{k}) = Z_{\beta\alpha}(\mathbf{k}), \quad Z_{xy}(\mathbf{k}) = Z_{yz}(\mathbf{k}) = Z_{zx}(\mathbf{k}) = 0, \quad (69)$$

and

$$Z_{xx}(\mathbf{k}) = Z_{yy}(\mathbf{k}). \quad (70)$$

Then (67) becomes

$$S_{\text{coh}}([\mathbf{Q}], \omega) = \frac{8\hbar n(\omega)A^2}{m} \text{Im} \left\{ x - x_t(\mathbf{k}) - c\epsilon x \times \left[1 - \frac{(1-c)C}{N} \sum_{\mathbf{k}} P_{xx}(\mathbf{k}) \alpha(\mathbf{k} - \mathbf{k}) \right]^{-1} \right\}^{-1}. \quad (71)$$

A measurement of the diffuse x-ray scattering intensity provides directly the short-range order function $\alpha(\mathbf{k})$, a half-bell-shaped curve. Equation (71) is then in the best form to use the x-ray data for a calculation of the inelastic neutron scattering. The contribution to the self-energy from each of the atoms correlated with a central defect can be seen by rewriting the convolution sum,

$$\frac{1}{N} \sum_{j' \mathbf{k}} \frac{\sigma_{x}^{j'}(\mathbf{k}) \sigma_{x}^{j'}(\mathbf{k})}{x - x_{j'}(\mathbf{k})} \alpha(\mathbf{k} - \mathbf{k}) = m \sum_l P_{0lxx} \alpha_l e^{i\mathbf{k} \cdot \mathbf{r}_l}. \quad (72)$$

In the Debye model of a monatomic crystal, the three branches are degenerate. By Eq. (6), then,

$$Z_{\alpha\beta}(\mathbf{k}) = \delta_{\alpha\beta} / \left(1 - \frac{\epsilon x}{N} \sum_{\mathbf{k}'} \frac{\rho(\mathbf{k} - \mathbf{k}')}{x - x(\mathbf{k}')} \right), \quad (73)$$

and $Z_{jj'}(\mathbf{k})$ is diagonal on j . Correlations among the defects introduce no branch mixing, and the neutron line shape may be represented by Eq. (63) with a self-energy

$$\Sigma^j(\omega) = c\epsilon [1 - (1-c)m\epsilon\omega^2 \sum_l P_{0lxx}(\omega) \alpha_l e^{-i\mathbf{k}^t(\omega) \cdot \mathbf{r}_l}]^{-1}. \quad (74)$$

Small-percentage shifts in peak frequency may be written as

$$\Delta\nu \approx \omega \Delta^j(\omega) / 4\pi \quad (75)$$

and the width in hertz as

$$\gamma = \omega \Gamma^j(\omega) / 2\pi. \quad (76)$$

In this continuous model the Brillouin zone is a sphere

¹⁹ E. C. Svensson and B. N. Brockhouse, Phys. Rev. Letters 18, 858 (1967).

of radius k_m and for the perfect-crystal Green's function

$$P_{0l\alpha\beta}(\omega) = \frac{3\delta_{\alpha\beta}}{mk_m^3} \int_0^{k_m} \frac{k^2 dk \sin(kr_l)}{[x - x(k)]kr_l}. \quad (77)$$

These functions are calculated in Appendix B in terms of $w \equiv \omega/\omega_m$.

The shift and the width of the inelastic coherent neutron scattering peaks can now be calculated if the short-range order parameters are known. The theory of Cowley²⁰ provides a set of coupled equations for the order parameters in terms of the interaction energies V between AA , AB , and BB pairs which are j th nearest neighbors. With the potential

$$kT_j \equiv \frac{1}{2}(V_{AA,j} + V_{BB,j}) - V_{AB,j} \quad (78)$$

and the function

$$L_\lambda = -\frac{1}{2}kT \ln \left\{ \frac{[c/(1-c) + \alpha_\lambda][(1-c)/c + \alpha_\lambda]}{(1-\alpha_\lambda)^2} \right\}, \quad (79)$$

the Cowley equations are

$$L_1 = T_1(1 + 4\alpha_1 + 2\alpha_2 + 4\alpha_3 + \alpha_4) + T_2(2\alpha_1 + 2\alpha_3 + 2\alpha_5) + T_3(4\alpha_1 + 2\alpha_2 + 4\alpha_3 + 4\alpha_4 + 4\alpha_5 + 2\alpha_6 + 4\alpha_7), \quad (80)$$

$$L_2 = T_1(4\alpha_1 + 4\alpha_3 + 4\alpha_5) + T_2(1 + 4\alpha_4 + \alpha_8) + T_3(4\alpha_1 + 8\alpha_3 + 8\alpha_7 + 4\alpha_{9b}), \text{ etc.} \quad (81)$$

The Cowley theory has worked remarkably well in predicting the short-range order parameters for Cu_3Au at temperatures above the ordering temperature. It seemed reasonable to try the theory at off-stoichiometric concentrations and to use the linear approximation

$$L_\lambda = \alpha_\lambda/c(1-c) \quad (82)$$

of Clapp and Moss,²¹ who have taken $T_1 = 450^\circ\text{K}$, $T_2 = -85^\circ\text{K}$, $T_3 = -20^\circ\text{K}$.²² The only parameter left in the theory, then, is the temperature T , which characterizes the state of short-range order in the system. This temperature is expressed in terms of the ratio T_c/T , where the critical temperature is given by

$$T_c = 8c(1-c)[T_1 - \frac{3}{2}T_2 + 2T_3] = 362^\circ\text{K}. \quad (83)$$

The order parameters initially computed from the linear theory seemed reasonable and small enough to justify the use of the linear theory, except for α_1 and α_2 . Using the linear theory for all other values of α_i , the first two Cowley equations were solved for α_1 and α_2 , which then took on reasonable values. The results for several values of T appear in Table I. The computed shifts and widths for the random and short-range ordered systems appear together with the experimental results in Figs. 2 and 3.

²⁰ Reference 12 and J. M. Cowley, Phys. Rev. **120**, 1648 (1960); **138**, A1384 (1965).

²¹ P. C. Clapp and S. C. Moss, Phys. Rev. **142**, 418 (1966).

²² S. C. Moss (private communication).

TABLE I. Short-range order parameters for $\text{Cu}_{0.907}\text{Au}_{0.093}$ characteristic of various temperatures.

λ	Site	$\alpha_\lambda(T_c/T=0.95)$	$\alpha_\lambda(T_c/T=0.9)$	$\alpha_\lambda(T_c/T=0.7)$
1	110	-0.0983	-0.0958	-0.0825
2	200	+0.291	+0.230	+0.1055
3	211	+0.0387	+0.0372	+0.0250
4	220	+0.0709	+0.0463	+0.0152
5	310	-0.0921 ^a	-0.0743	-0.0282
6	222	-0.0344	-0.0304	-0.0141
7	321	+0.0002	+0.0002	-0.0007
8	400	+0.1126	+0.0729	+0.0197
9a	330	-0.0431	-0.0245	-0.0043
9b	411	+0.0367	+0.0262	+0.0083

^a The value of α_5 for $T_c/T=0.95$ has been reduced by 10% to compensate approximately for errors in the linear theory.

VI. IMPURITY BAND

If a single light impurity is substituted for a host atom in a crystal, a mass defect theory predicts a localized mode at a frequency ω_L given by

$$1/\epsilon = \omega_L^2 m P_{00}(\omega_L). \quad (84)$$

Interactions among the defects, however, broaden the localized mode into a band. In order to demonstrate the possible effects of correlations among the defects on the width of this impurity band, we consider a clustering correlation in which those sites which are nearest neighbors of a defect (in the shell $\lambda=1$) have a probability of being occupied by a defect which is higher than the concentration. It is assumed that the defect deficiencies, required to make the total concentration equal to c , are widely dispersed throughout the crystal.

In the Debye approximation, Eq. (20) may be written in a self-energy form to give

$$\langle G_{00\alpha\beta}(\omega) \rangle = \frac{1}{mN} \sum_{\mathbf{k}} \frac{\delta_{\alpha\beta}}{\omega^2 - \omega^2(\mathbf{k}) - c\epsilon\omega^2\{1 - m\epsilon\omega^2(1-c)\sum_l P_{0lxx}\alpha_l e^{i\mathbf{k}\cdot\mathbf{r}_l}\}^{-1}}. \quad (85)$$

The values of ω for which this function is singular, and hence has a finite imaginary part, constitute the impurity band. The lowest such frequency ω_b is that which makes the denominator vanish for $\omega(\mathbf{k})=0$, the highest, ω_u , for $\omega(\mathbf{k})=\omega_m$.

$$m\omega_b^2 \sum_l P_{0l}(\omega_b)\alpha_l = \frac{1-c\epsilon}{(1-c)\epsilon}, \quad (86)$$

$$m\omega_u^2 \sum_l P_{0l}(\omega_u)\alpha_l e^{i\mathbf{k}_m\cdot\mathbf{r}_l} = \left[1 - \frac{c\epsilon\omega_u^2}{\omega_u^2 - \omega_m^2} \right] \frac{1}{\epsilon(1-c)}, \quad (87)$$

where $\alpha_0=1$, and otherwise for this example only $\alpha_{\lambda=1}$ can be nonzero.

If $\alpha_{\lambda=1}$ is set equal to zero, the result of ET, for uncorrelated defects, is obtained. In this case the left-hand sides of Eqs. (86) and (87) are the same, and are plotted as curve R in Fig. 4. The right-hand sides are

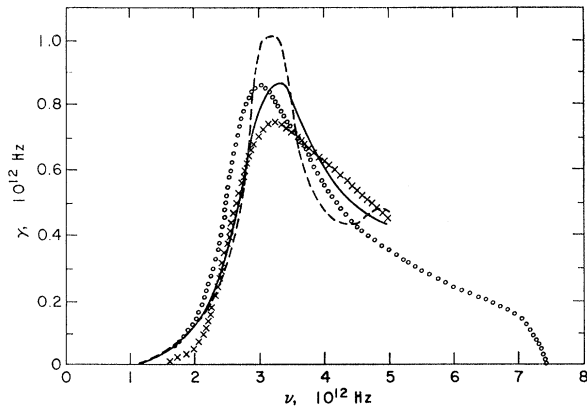


FIG. 3. The widths of the neutron scattering peak at frequency ν for $\text{Cu}_{0.907}\text{Au}_{0.093}$ as calculated in the Debye model for random defects (dotted curve), ten shells of defects at characteristic temperature $T=T_c/0.95$ (dashed curve), two shells of defects at $T=T_c/0.95$ (solid curve). The xxx are the data of Svensson *et al.*, corrected for the additional mosaic spread of the impure crystal.

plotted for $\epsilon=0.448$, $c=0.05$ and 0.10 , and for $\epsilon=0.823$, $c=0.033$. These values correspond to the systems Pd:Ni and V:Be studied by incoherent inelastic neutron scattering.^{23,24} The intersections of a horizontal (low-frequency) line, marked by the concentration, with the R curve occur at the lowest frequency in the random-impurity band. The intersection of the curved (high-frequency) line with R gives the highest frequency, and the intersection of R with the horizontal $1/\epsilon$ line gives the single-defect local-mode frequency that, for this theory, lies near the middle of the band.

Both the Debye theory and the neglect of force-constant changes tend to predict a local-mode frequency which is too high, in this case by as much as 30% for V:Be. The predicted widths for the random theory given in Table II are much smaller than the widths that might be inferred from the experimental results.

If a nonzero value of $\alpha_{\lambda=1}$ is used, the left-hand sides of Eqs. (86) and (87) are represented by two lines which may be calculated from the Debye-model Green's functions given in the last section and in Appendix B.

The body-centered V:Be is approximated with a value of $f \equiv k_m r_l / \pi = 1.35376$ for l in the $\lambda=1$ shell of only eight atoms. In Eq. (87), $\sum_l e^{i k_m \cdot r_l}$ is replaced by $\sum_l \sin(k_m r_l) / k_m r_l$, and not by its most negative value.

For a positive value of $\alpha_{\lambda=1}$, approximating very crudely the clustering of light defects, the left-hand sides of Eqs. (86) and (87) for low and high frequencies are, respectively, below and above the random curve, and give new limits to the impurity band. A positive $\alpha_{\lambda=1}$, then, is seen to widen the band, whereas a negative $\alpha_{\lambda=1}$, representing a mutual avoidance among the light defects, would decrease the bandwidths, as might have

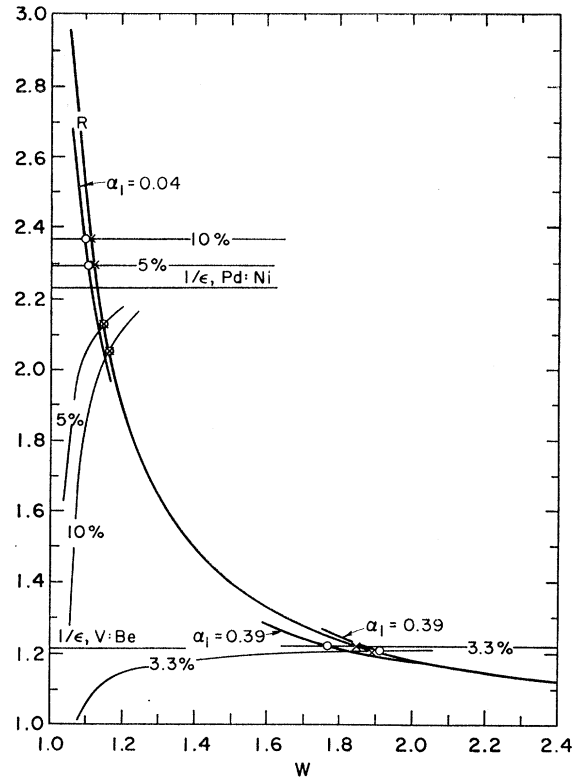


FIG. 4. Impurity-band limits for Pd:Ni and V:Be. The curve R for random defects intersects (X) the low- (horizontal) and high- (curved) frequency lines from Eqs. (86) and (87) to give the limits of the impurity band for the concentrations indicated. The intersection of R with $1/\epsilon$ gives the local-mode frequency. The lines adjacent to R marked with nonzero values of $\alpha_{\lambda=1}$ give low and high impurity-band limits, indicated by the encircled intersections for defect clustering. For Pd:Ni, the curve for the high-frequency limit for $\alpha_{\lambda=1}=0.04$ is indistinguishable on this scale from the R curve and has not been drawn.

been expected from simple physical arguments. Furthermore, for very light impurities with high local-mode frequencies, *unrealistically high* values of $\alpha_{\lambda=1}$, such as $\alpha_{\lambda=1}=0.39$ for V:Be, are required to produce any appreciable broadening. For the relatively heavier Ni impurity in Pd, however, appreciable broadening is produced by values of $\alpha_{\lambda=1}$ that are quite possible for the fairly high defect concentrations studied experimentally. This result also seems physically reasonable; the lighter defect vibrations are more localized, and are thus less affected by the neighbors than are the vibrations of

TABLE II. Local mode frequencies and calculated impurity bandwidths.

Alloy	w_L (Debye)	w_L (expt)	$\alpha_{\lambda=1}$	Δw
$\text{V}_{0.967}\text{Be}_{0.033}$	1.87	1.3–1.6	0	0.045
$\text{Pd}_{0.95}\text{Ni}_{0.05}$	1.13	1.10	0.39	0.137
			0	0.028
			0.04	0.048
$\text{Pd}_{0.9}\text{Ni}_{0.1}$			0	0.056
			0.04	0.067

²³ B. Mozer, K. Otnes, and V. W. Myers, Phys. Rev. Letters **8**, 278 (1962).

²⁴ B. Mozer, K. Otnes, and C. Thaper, Phys. Rev. **152**, 535 (1966).

relatively heavier light defects with a local-mode frequency closer to the perfect-crystal band. But, although the effects of this type of short-range order on the impurity bandwidth appear reasonable, the entire theory is too simple to account realistically for the widths, as ET has suggested.

If the incoherent neutron scattering lengths of defect and host atoms are different, there is an additional contribution, proportional to c , to that part of the incoherent scattering given by Eq. (60). For the Debye model,

$$G_{00xx}^d(\omega) = \frac{c}{mN} \sum_{\mathbf{k}} \{ [\omega^2 - \omega^2(\mathbf{k})] \times [1 - (1-c)m\epsilon\omega^2 \sum_l P_{0l}(\omega)\alpha_l e^{i\mathbf{k} \cdot \mathbf{r}_l}] - c\epsilon\omega^2 \}^{-1}, \quad (88)$$

which has a finite imaginary part over the same range of high frequencies as does $\langle G_{00xx}(\omega) \rangle$.

VII. DISCUSSION

The approximation (15), which is central to the theory developed above, is valid only for small defect concentrations. Furthermore, validity of the multiplicative aspect of this approximation requires that the short-range order be a perturbation on the random distribution of defects. This may indeed be the case for many real alloys at small defect concentrations for which one could expect the various $|\alpha_l|$ to increase no faster than c with increasing concentration. For such an alloy, the multiplicative aspect of (15), which arises only in terms of (11) with three or more different defects, then results in errors of order c^3 or higher. Alternatively, one could say that, at low concentrations, $c\rho_{l_1 l_2 l_3}$ is expected to deviate from its random value of c^3 for $l_1 \neq l_2 \neq l_3 \neq l_1$ by a value no greater than c^3 .

A more serious error would seem to result from the asymmetrical nature of (15), which causes an improper weighting of all crossed graphs. Any term of the general form (17) which is underweighted by a factor c^b in the random case will be underweighted when defect sites are correlated by the factor

$$[c + (1-c)\alpha_{l_1-l_2}]^{b_1} [c + (1-c)\alpha_{l_2-l_3}]^{b_2} \cdots [c + (1-c)\alpha_{l_{n-1}-l_n}]^{b_{n-1}}, \quad (89)$$

where $b_1 + b_2 + \cdots + b_{n-1} = b$. If the quantities $|\alpha_{l_i-l_j}|$ rise more slowly than c with increasing defect concentration, the errors made in both random and short-range ordered cases are equivalent. For the 9.3 at.% defect concentration system studied, however, $|\alpha_l|$ is not always less than c , especially for $\lambda=2$, and one must conclude that this concentration is somewhat too high for the theory to be valid.

The theory is less satisfactory for the short-range order parameters themselves. In the random theory, all graphs corresponding to a single defect should be weighted by c , those corresponding to a pair should be

weighted by c^2 , etc. For the short-range ordered case, a single defect should have a factor c , pairs a factor $c\varrho$, triples a factor $c\varrho\varrho$, etc. First-order terms in ϱ then come from pairs. In our approximation, however, crossed pair graphs are weighted by factors $c\varrho\varrho$, $c\varrho\varrho\varrho$, etc.; only uncrossed pair graphs contribute to the linear dependence on ϱ . Generally, one can say that this theory is approximate to n th order in the short-range order parameters to the extent that the ET theory is approximate to $(n+1)$ th order in the concentration. Solutions to the random pair defect problem do appear in unpublished works,^{25,26} but the resulting expressions are too cumbersome to be readily used in physical calculations.

In order to compare the predictions of this theory with experimental results such as the shifts and widths of the coherent inelastic neutron scattering peaks, an experimentally determined $\alpha(\mathbf{k})$ should be used to calculate $Z(\mathbf{k})$. One cannot expect very good agreement with experiment if α_l is used for $\lambda_{\max}=10$, as was done here for want of an experimental $\alpha(\mathbf{k})$. The short-range order parameters for $\lambda>10$ are probably not negligible, as was shown for disordered Cu_3Au by Moss's theoretical reconstruction of the $\alpha(\mathbf{k})$ from the first ten shells of α_l and subsequent comparison with the experimental $\alpha(\mathbf{k})$ from which the α_l were derived.²⁷ In our case, the corrections to the self-energy are products of the α_l and perfect-crystal Green's functions which fall off with distance only as $1/\sqrt{r_l}$ within the band of perfect-crystal frequencies. Corrections from shells beyond $\lambda=10$ would be important. That the shifts and widths calculated from the first two order parameters approach the experimental results slightly better than do those calculated with ten parameters is, therefore, not disturbing, although it is somewhat surprising.

The shift and width curves are rather sensitive to the model used for the perfect crystal and the use of the Debye model, which greatly simplifies the calculation, cannot be justified. As usual, the Debye model overestimates the defect resonance frequency, an error that makes the random mass defect theory (and perhaps the short-range-ordered theory) appear to come closer to the experiment than it should. Although this theory is very crude, it is the logical extension to a short-range-ordered defect system of the simplest defect theory capable of producing analytically such physical features as a shift and a width of neutron scattering peaks and an impurity band; it may be a reasonable first step towards an understanding of the effect of short-range order on the dynamics of imperfect three-dimensional crystals.

Note added in proof. The defect-correlation-function approach may also be used with force-constant changes. By techniques similar to those of Appendix A, we may

²⁵ A. A. Maradudin, Westinghouse Research Laboratories Scientific Paper No. 63-129-103-P9, 133, 1963 (unpublished).

²⁶ K. Lakatos, thesis, Cornell University, 1967 (unpublished).

²⁷ S. C. Moss, J. Appl. Phys. **35**, 3547 (1964).

demonstrate (ET) Eqs. (3.6) and (3.7) for general defects in the random limit provided that Eq. (3.7) is taken as a definition of $X_{jj'}(\mathbf{k}, \omega)$.

ACKNOWLEDGMENTS

The author is grateful to Dr. J. M. Rowe for a discussion which led to this problem and to Professor R. J. Elliott, Professor D. W. Taylor, and Professor B. Goodman for critical readings of this report. Dr. A. Rahman, Dr. L. Guttman, Dr. L. Schwartz, and other members of the Argonne Solid State Science Division provided suggestions and encouragement. The author is particularly indebted to Professor S. C. Moss for calculating the initial sets of short-range order parameters and for discussions.

APPENDIX A: RANDOM LIMIT

Elliott and Taylor sum Eq. (2) by first selecting all terms involving only one defect (Fig. 1, (a), (c), (h), etc.) and applying corrections in order to re-include in those sums of more than one defect some terms in which two or more defect position indices are the same. After extending this procedure to all numbers of defects and applying a configuration average, they find, for a monatomic crystal with mass defects,

$$\langle \mathbf{G} \rangle = \mathbf{P} + c \mathbf{P} \mathbf{X}' \langle \mathbf{G} \rangle, \quad (\text{A1})$$

where

$$\mathbf{X}' \equiv \mathbf{C} [1 - (1-c) \mathbf{C} \mathbf{P}_{00}]^{-1}. \quad (\text{A2})$$

We show that this result is obtained from the defect-correlation-function approach with approximation (15) in the random limit, where

$$c p_{i_1 i_2 \dots i_n}^{\text{RL}} = c (c + (1-c) \delta_{i_1 i_2}) (c + (1-c) \delta_{i_2 i_3}) \dots (c + (1-c) \delta_{i_{n-1} i_n}). \quad (\text{A3})$$

Mechanically summing terms (17), exhibiting explicitly terms up to fourth order, gives

$$\begin{aligned} \langle \mathbf{G} \rangle = & \mathbf{P} + c \mathbf{P} \mathbf{C} \mathbf{P} [1 + (1-c) \mathbf{C} \mathbf{P}_{00} + (1-c)^2 \mathbf{C}^2 \mathbf{P}_{00}^2 \\ & + (1-c)^3 \mathbf{C}^3 \mathbf{P}_{00}^3 + \dots] \\ & + c^2 \mathbf{P} \mathbf{C} \mathbf{P} \mathbf{C} \mathbf{P} [1 + 2(1-c) \mathbf{C} \mathbf{P}_{00} + 3(1-c)^2 \mathbf{C}^2 \\ & \times \mathbf{P}_{00}^2 + \dots] \\ & + c^3 \mathbf{P} \mathbf{C} \mathbf{P} \mathbf{C} \mathbf{P} \mathbf{C} \mathbf{P} [1 + 3(1-c) \mathbf{C} \mathbf{P}_{00} + \dots] \\ & + c^4 \mathbf{P} \mathbf{C} \mathbf{P} \mathbf{C} \mathbf{P} \mathbf{C} \mathbf{P} \mathbf{C} \mathbf{P} [1 + \dots] \\ & + \dots. \end{aligned} \quad (\text{A4})$$

The first term (unity) in the first (second, ...) bracket represents a sum over all possible graphs of one defect to first order (two defects to second order, ...). The following terms in a square bracket, which corresponds to a certain number of defects, are corrections to brackets involving more defects. These corrections are necessary because two or more defect-site indices may be the same. However, the corrections are only made for the uncrossed graphs, and the crossed graphs are allowed

TABLE III. The number of graphs of different kinds in the expansion of Eq. (2).

Order	Uncrossed graphs						Defects						All graphs					
	1	2	3	4	5	6	7	1	2	3	4	5	6	7	8	9	10	11
1	1							1										
2	1	1						1	1									
3	1	2	1					1	3	1								
4	1	3	3	1				1	7	6	1							
5	1	4	6	4	1			1	15	25	10	1						
6	1	5	10	10	5	1		1	31	90	65	15	1					
7	1	6	15	20	15	6	1	1	63	301	350	140	21	1				

to fall where they may, improperly weighted but not omitted. The coefficients of the corrections are those of the expansion of $[c + (1-c)\delta_{il}]\delta_{il}$ and form a Pascal's triangle (shown in the left triangular half of Table III). The entries correspond simply to the number of uncrossed graphs for a given number of defects to a given order. For comparison, the total number of graphs is given in the right triangular half of Table III.

The first square bracket in (A4) can be summed to $[1 - (1-c) \mathbf{C} \mathbf{P}_{00}]^{-1}$, the second to $[1 - (1-c) \mathbf{C} \mathbf{P}_{00}]^{-2}$, and the n th to $[1 - (1-c) \mathbf{C} \mathbf{P}_{00}]^{-n}$. Then using the definition (A2) we have

$$\langle \mathbf{G} \rangle = \mathbf{P} + c \mathbf{P} \mathbf{X}' \mathbf{P} + c^2 \mathbf{P} \mathbf{X}' \mathbf{P} \mathbf{X}' \mathbf{P} + c^3 \mathbf{P} \mathbf{X}' \mathbf{P} \mathbf{X}' \mathbf{P} \mathbf{X}' \mathbf{P} + \dots, \quad (\text{A5})$$

which is equivalent to (A1).

APPENDIX B: CALCULATION OF DEBYE-MODEL GREEN'S FUNCTIONS

In order to calculate the Green's functions (77), we introduce the parameter

$$w \equiv k/k_m = \omega/\omega_m \quad (\text{B1})$$

and the lattice parameter a for the fcc unit cell of four atoms. Then

$$r_l = a(\frac{1}{2}\lambda)^{1/2}, \quad (\text{B2})$$

and from the relation between the volumes of the unit cell and of the Brillouin zone,

$$v_k = (2\pi)^3/v_l, \quad (\text{B3})$$

we have that

$$k r_l = \pi w f \sqrt{\lambda}, \quad (\text{B4})$$

where

$$f = \sqrt{2}(3/\pi)^{1/3} = 1.39264. \quad (\text{B5})$$

For $l=0$, therefore,

$$\text{Im} P_{00\alpha\beta}(\omega) = \frac{3\pi w}{2m\omega_m^2} \delta_{\alpha\beta} \quad (w < 1) \quad (\text{B6})$$

$$= 0, \quad (w \geq 1)$$

$$\text{Re} P_{00\alpha\beta}(\omega) = \frac{3\delta_{\alpha\beta}}{2m\omega_m^2} \left\{ w \ln \left| \frac{1+w}{1-w} \right| - 2 \right\}. \quad (\text{B7})$$

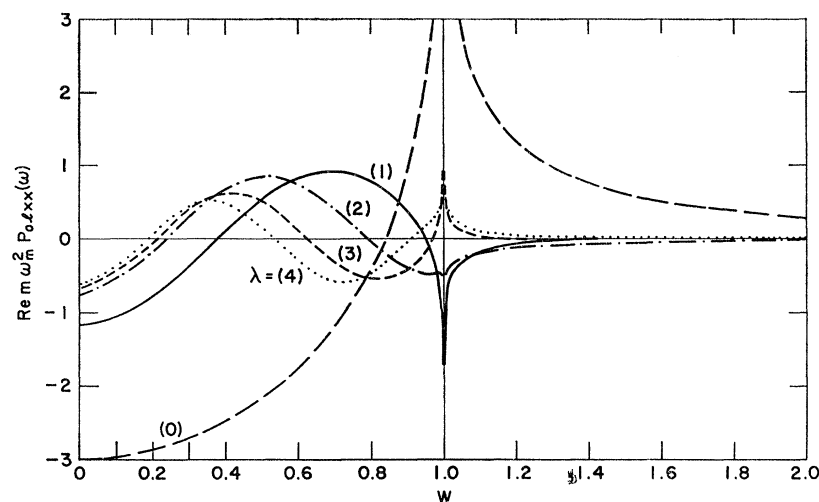


FIG. 5. The real parts of the perfect-crystal Green's functions in the Debye model for the atomic displacement auto-correlation and for displacement correlations between a central atom and atoms in the first four shells (λ) of its neighbors. The coordinate $w \equiv \omega/\omega_m$. Oscillations at high frequency are too small to be seen on this scale.

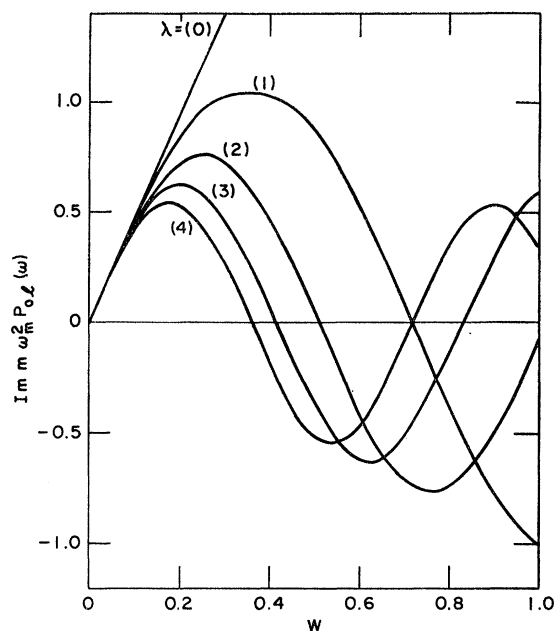


FIG. 6. The imaginary parts of the perfect-crystal Green's functions of Fig. 5: Debye model. All imaginary parts are zero for $w \equiv \omega/\omega_m > 1$.

For $l \neq 0$,

$$P_{0l\alpha\beta}(\omega) = \frac{3\delta_{\alpha\beta}}{m\omega_m^2\pi f\sqrt{\lambda}} \int_0^1 \frac{w'dw'}{w^2 - w'^2} \sin(\pi f w' \sqrt{\lambda}), \quad (\text{B8})$$

$$\begin{aligned} \text{Im} P_{0l\alpha\beta}(\omega) &= \frac{3\delta_{\alpha\beta}}{2m\omega_m^2\pi f\sqrt{\lambda}} \sin(\pi f w \sqrt{\lambda}), \quad (w < 1) \\ &= 0, \quad (w \geq 1) \end{aligned} \quad (\text{B9})$$

$$\begin{aligned} \text{Re} P_{0l\alpha\beta}(\omega) &= \frac{3\delta_{\alpha\beta}}{2m\omega_m^2\pi f\sqrt{\lambda}} \{ \sin(\pi f w \sqrt{\lambda}) \\ &\times [\text{Ci}(\pi f(1+w)\sqrt{\lambda}) - \text{Ci}(\pi f(1-w)\sqrt{\lambda})] \\ &- \cos(\pi f w \sqrt{\lambda}) [\text{Si}(\pi f(1+w)\sqrt{\lambda}) \\ &+ \text{Si}(\pi f(1-w)\sqrt{\lambda})] \}, \quad (\text{B10}) \end{aligned}$$

where Si and Ci are the sine and cosine integral functions. The real and imaginary parts of these functions for $\lambda = 0, 1, 2, 3, 4$ are plotted in Figs. 5 and 6. The logarithmic singularities at $w = 1$ are a feature of the Debye model and would not occur for a more realistic density of states.

The self-energy of Eq. (74) still depends on the momentum transfer vector through $\exp(i\mathbf{k} \cdot \mathbf{r}_l)$. For the transverse branches under study, we may apply a simple nearest-neighbor central-force model for which

$$\kappa_l(\omega) = (4/a) \arcsin(w\sqrt{2}). \quad (\text{B11})$$